TD-DFT Investigation on Anion Recognition Mechanism of Anthraldehyde based Fluorescent Thiosemicarbazone Derivatives

Sabeel M Basheer (sabeelmb@gmail.com)
VIT-AP Campus
Rohini Gandhaveeti
NIT-Tiruchirappalli: National Institute of Technology Tiruchirappalli

Research Article

Keywords: TDDFT, TS, NBO, PES, ESPT

Posted Date: April 15th, 2022

DOI: https://doi.org/10.21203/rs.3.rs-1513040/v1

Abstract

The mechanism of host-guest interaction of receptors towards fluoride ion has been investigated using computational methods. To distinguish the effect of aromaticity in host-guest interaction, we investigated unsubstituted (ATSC) and phenyl substituted (APTSC) anthracene thiosemicarbazones towards different ions. In the ground state of receptor-fluoride complex, the added fluoride ion made hydrogen bond through N–H … F … H–N. Whereas, the intramolecular hydrogen bonding was through F–H … N in the excited state of receptor-fluoride complex. Experimental absorption and emission spectra were well reproduced by the calculated vertical excitation energies. The transition state (TS) calculations were performed to understand the thermodynamic features and mechanism of host-guest interaction. The natural bond orbital analyses show the second perturbation energy for donor-acceptor interaction of F - with hydrogen is more than 300 kcal/mol at the excited state of receptor-fluoride complex, which indicates the strong single bond between fluoride and hydrogen atom. The PES scan confirms that deprotonation took place at the excited state of receptor-fluoride complex. The results indicate that the excited-state proton transfer (ESPT) process from N–H group nearby the anthracene moiety. The APTSC is better chemosensor than ATSC. This infer that the aromaticity will increase the efficiency of fluorescence receptor towards fluoride ion.

1. Introduction

In view of the fact that ions play a major role in many chemical and biological process, designing ion selective molecular sensors is a challenging entity in supramolecular chemistry [1,2]. Fluoride ion is a necessary trace element in the human body, which has vital role in a broad range of chemical, biological and environmental processes [3-5]. The excessive absorption of fluoride ion can cause fluorosis of bone, immune system disruption, urolithiasis, kidney damage and cancer [6]. It has one of the most perplexing ion recognition, due to its high electronegativity and hydration enthalpy [7]. The detection of fluoride ion can prevent and cure dental problems and osteoporosis [8]. There are many experimental reports as molecular optical sensors, while very few reports of selective fluorescence fluoride sensor is seen, due to the surface charge density and similar basicity of fluoride ion with other ions [9-12].

The theoretical characteristic and the detailed investigation of host-guest mechanism is perilous for fluorescent chemosensor. Based on the experimental results, researchers have proposed several categories of signalling mechanisms for fluoride chemosensor, such as photo-induced electron transfer (PET), intramolecular charge transfer (ICT), excimer and exciplex formation, metal ligand charge transfer (MLCT), excited-state intramolecular proton transfer etc. [13-16]. Among these, the ESPT performing dynamic role in determining the photophysical and photo-chemical properties of organic molecules, which usually shows dual fluorescence behaviour [17,18]. The PET mechanism was used to describe the hydrogen bonding, in which enhancing or quenching corresponds to red or blue shifts in the absorption spectra [19-21]. Iverson and others demonstrated that charge transfer and π-π stacking interactions between a colourless guest and electron rich aromatic rings produce coloured donor-acceptor complexes [22].

Among the chemosensors, fluorescent chemosensors have many advantages such as ease of detection, low cost, high sensitivity and biologically appropriate diagnostic tools. Recently, Udayakumari et. al., reported APTSC as selective chemosensor for fluoride ion over other anions [23]. Taking this system as an example, herein we investigated the sensing mechanism of fluoride ion theoretically. The sensing mechanism of ATSC receptor was also investigate to evaluate the effect of aromatic group in sensing process. By using computational methods, we investigated the host-guest interaction of fluorescent thiosemicarbazones with anthraldehyde as receptors, which contain electron rich aromatic rings. Further, by comparing the results, we suggested that the aromaticity of the receptor will enhance the chemosensing behaviour.

2. Computational Methods

The hybrid density functional theory (DFT) and Time Dependent DFT (TD-DFT) calculations were performed using Gaussian 09 program. Optimizations have been carried out without symmetry constraints. The ground state of the receptors, receptor-fluoride complexes and deprotonated receptors were optimized using the hybrid B3LYP functional with 6-31G(d,p) basis set. Whereas, the optimization of excited state geometries were calculated using Handy and co-workers long range modified version of B3LYP casted as Coulomb-attenuating method (CAM) hybrid function with long-range corrections (CAM-B3LYP) [24]. The vertical state excitation calculations were employed for the calculation of excitation state. The Polarised Continuum Model (PCM) with dimethyl sulfoxide solvent (Dielectric constant = 46.826) calculation was implemented throughout the steps to include the solvent effect. To verify the ground state and excited state optimized geometries are in local minima, the vibrational frequency calculations were run for all the optimized structures. In order to understand and verify the nature of transition state and intermediate structures, the transition state (TS) and intrinsic reaction coordinate (IRC) calculations were carried out. The natural bond orbital (NBO) analyses were carried out at ground state and excited state structures of receptor-fluoride complexes to understand the charge distribution and energy of bonding and anti-bonding orbitals. The second order Fock matrix calculations were carried out to estimate the host–guest interactions [25,26]. The ESPT mechanism was confirmed with potential energy surface (PES) analysis [27].

3. Results And Discussion

3.1 Geometric studies

To examine the sensing process for fluoride anion, the ground state and excited state geometries of the chemosensors (APTSC and ATSC), receptor-fluoride complex have been investigated in detail. The optimized geometric structures of APTSC and ATSC receptors and receptor-fluoride complexes (APTSC–F and ATSC–F) at the ground state and excited state are as shown in **Figure 1** and **Figure 2**. The important structural parameters of ATSC and APTSC are listed in **Table 1** and **Table 2**. The vibrational frequency of the ground state structures were positive, hence, all the structures are in local minima. The ground state

energies of ATSC and APTSC are -43.34 and -51.824 eV kcal/mol respectively. Whereas, the receptor-fluoride complex such as APTSC–F and ATSC–F have less SCF energy than pure receptor.

In the ground state of APTSC, the dihedral angle between C5–C4–N3–N2 was 34.39^{o}. The dihedral angle between anthracene moiety and imine group were115.99 and 1.248 for APTSC and ATSC receptors respectively. These results revealed that the receptors, APTSC and ATSC were not in coplanar. The N1–H1 and N2–H2 bond distance in APTSC are found to be 1.01 and 1.02 Å respectively. The bond angle between C1-N1-C2 is 130.90^{0}. The C-N bond distance in the APTSC is 1.28 Å. However, in the case of excited state of APTSC-F complex, the C-N bond distance found 1.32 Å, The high bond length points the formation of single bond between C-N. In the ground state of receptor-fluoride complex, the bond distance between F-H1 and F-H2 were found in the range of 1.50 and 1.46 Å, which indicated that the fluoride ion made hydrogen bond with receptor *via* N–H···F···H–N. The dihedral angles between phenyl group, imine group and anthracene moiety- imine group were found same in the APTSC and APTSC-F complex.

In the excited state of APTSC-fluoride (APTSC-F*) complex, the calculated dihedral angle between anthracene moiety and imine group is 159.81, which is higher than the ground state structure of APTSC-F complex. In the APTSC-F*, the bond distance between F–H1 and F–H2 are found to be 1.91 and 0.99 Å respectively. The lower bond length between fluoride and H2 implies the presence of strong bond between them, which indicates the proton transfer was happened at excited state. While, in the case of excited state ATSC–F (ATSC–F*) structure, the F–H1, F–H2, N–H1 and N–H2 bond distance are calculated as1.97, 1.05, 1.01 and 1.40 Å respectively. The higher bond distance between N-H2 and lower bond distance between F-H2 implies the deprotonation happened first at ‘H2’ proton of ATSC. Hence, it is evident of the excited state proton transfer (ESPT) process. The dihedral angle between anthracene moiety and imine group was twisted to 28.680^{0} in ATSC–F*, which provides higher planarity and conjugation than pure receptor. The extension of the conjugation might help to delocalize the negative charge of the fluoride ion, hence, the photophysical property of the receptor-F complex varies from pure receptor.

3.2 Absorption and molecular orbital analysis

The absorption spectral studies were carried out for receptors and receptor-fluoride complexes to understand the change in optical behaviour in the host-guest process. The molecular orbitals involved in the major electronic transitions with the largest oscillator strength have been shown in **Figure 3** and **Figure 4**. Theoretical calculations predict six absorption transitions for each compounds, and the dominant absorption transition of APTSC, APTSC-F complex, ATC and ATSC-F complex are given in **Table 3** and **Table 4**. The intense absorption transition for APTSC is calculated at 367.48 nm, with large oscillating strength 0.2957, which is assigned as π→π* transition from the highest occupied molecular orbital (HOMO, H) to the lowest unoccupied molecular orbital (LUMO, L). In HOMO, the electron delocalized over anthracene moiety and imine group. Whereas, in LUMO, the electron cloud only delocalized at anthracene moiety. The second dominant absorption peak was at 310 nm, which was corresponds to HOMO, third lowest unoccupied molecular orbital (LUMO+2, L+2), where the electron delocalized throughout the anthracene moiety. While in APTSC-F complex, the absorption peak at 367 nm

decreases and accompanies with the formation of a new band at 374 nm. The high oscillating strength and percentage π→π* transition was between HOMO to LUMO. In the HOMO of APTSC-F complex, the electron was delocalized only on imine group. Whereas, the electron was delocalized on anthracene moiety in LUMO.

In the case of ATSC, the high oscillated frequency wavelength at 411 nm with 3.0136 eV energy. The high percentage orbital transition was in between HOMO-1 to LUMO. The second major absorption transition was at HOMO to LUMO orbitals. In HOMO, the electrons delocalized in anthracene moiety and thiosemicarbazide group. While, the HOMO-1 and HOMO-2 orbitals had electron cloud only on imine group, not in anthracene moiety. Whereas, in LUMO, LUMO+1 and LUMO+2 orbitals the electron clouded only at anthracene moiety. The resulting electron cloud rearrangement is cause for the changes in the photophysical properties of receptor in the host-guest interaction. **Figure 5** displays the calculated orbital energies of APTSC and APTSC-F complex. The energy gap between HOMO and LUMO orbitals in emission profile is higher than that of absorption profile. The complete charge separation from thiosemicarbazone group to anthracene in the relaxation process is in good accordance with the definition of PET. The absorption profiles are calculated using the Gaussian models and compared with the experimental results.

3.3 Transition state calculations

In order to capture the dynamics feature of the sensing process, we evaluated the Gibbs free energy profile in DMSO medium. The transition state and intermediate structures were calculated, which are as shown in **Figure 6** and **Figure 7**. In the transition state and intermediate structures, the fluoride ion interacts with receptor via hydrogen boning. The relaxation of the transition state toward the intermediate and the products by IRC calculations did not detect any intermediates, which revealed that the host-guest process is S_N2 type of reaction. The sensing process of ATSC and APTSC with fluoride ion had the free energy (ΔG) of 177.17 and 186.22 kcal/mol. The more negative value of ΔG was the reason for quick response of APTSC than ATSC towards fluoride ion. In the transition state, the bond distance between fluoride ion and N2-H2 and F-H2 were about 1.45 and 1.02 Å, which revealed the fluoride ion has higher hydrogen bond with hydrogen atom than in ground state and results the transition state in higher energy state. The binding constant (K_a) of the receptor (APTSC and ATSC) with fluoride ion was calculated ($\ln K_a = \frac{-\Delta G}{RT}$, where, R, T and K_a are the universal gas constant, temperature and the binding constant respectively). The binding constant of APTSC and ATSC towards fluoride ion found to be 0.930 and 0.927 M^{-1} respectively.

Natural Bond orbital (NBO) calculation

Natural bond orbital (NBO) analysis provides the most accurate possible ‘natural Lewis structure’ picture, because all orbital details are mathematically chosen to include the highest possible percentage of the electron density. Further confirming the ESPT process and the deprotonation of H2 from receptor via

hydrogen bond, the NBO analysis were carried out at the ground state and excited state of receptor-fluoride complex. The binding energy (ΔE) between of binding sites of fluoride ion and the residue for receptor were plays an important role in revealing the ability for fluoride anion to attach proton. The binding energies between the two segments separated by H1–F and H2–F of receptor-fluoride complexes were calculated.

The natural atomic hybrids calculation gave the bond order on each hybrid atoms. The hybridisation with single bond between N25–H41 and N27–H42 were listed in **S3**. In ground state APTSC-F complex, sp^3 nitrogen was hybridised to 's' hydrogen, but this bond was not in excited state. Resulting, a strong host–guest interaction between fluoride ion and APTSC occurred, which can be treated by the second-perturbation energy E(2). The interaction between host and guest can be explained by using second perturbation energy, which has been calculated using the equation, $E(2) = \Delta E = \frac{q_i F_{ij}^2}{\varepsilon_j - \varepsilon_i}$, where E(2) is the second perturbation energy, F_{ij} is the off-diagonal element in the NBO Fock matrix, q_i is the donor orbital occupancy, and ei and ej are orbital energies. The NBO characters in ground state and excited state were given in the **Table 5.** The σ-σ* and n-σ* host-guest interactions were seen at the ground state and excited state of ATSC–F and APTSC–F complexes. In the ground state, two mode of interactions were presented *via* fluoride to N25–H41 and N27–H42. Whereas, in the excited state had only one interaction, which was *via* fluoride ion with H41. In the ground state of receptor-fluoride complex, the second perturbation energies were varies from 0.3 to 44 kcal/mol, which revealed that both the receptor make hydrogen bonding with fluoride ion in the ground state. But, in the excited state of receptor-fluoride complexes have LP(F)→LP*(H41) interaction with more than 300 kcal/mol energy, which show the fluoride ion has make strong bond with H(41) proton. This interaction generated from lone pair electron (n) of fluoride ion to n* of hydrogen (H41). The interactions were generated from core electron and lone pair electron. More overlap of the electron density confirms the strong donor-acceptor interactions, due to this, the H(41) preferred to interact with Fluoride ion rather than H(43).

3.4 Potential energy curve of excited state geometry

To confirm the ESPT mechanism in host-guest interaction, the potential energy curve investigation of the ground state and excited state receptor-fluoride had been evaluated. The PES calculations employed with only varying the N-H bond length from 0.90 to 1.80 Å in steps of 0.05 Å, which can provide qualitative energetic pathways for the ESIPT process. In the case of APTSC-F complex, the bond distance between N(25)–H(42) and N(27)–H(43) at ground stat and excited state where N(25) is at nearby anthracene moiety and (N27) is nearby Phenyl group. The less energy was seen for the excited state N(25)–H(42) bond distance at 1.00 Å, and the same at ground state was more stable at 1.10 Å bond distance. These results confirm that the fluoride ion form an intermolecular hydrogen bond with receptor's nitrogen (N2), which is the NH proton near by the anthracene moiety. In the host-guest interaction, the fluoride ion was first react with receptor and form hydrogen bond *via* N–H···F, not in free H^+ ion. Hence, it show a red shift in the fluorescence emission spectra and UV absorption spectra. This change in fluorescence colour

signal can directly detect with the naked eye. The PES curve of APTSC-F and ATSC−F complex in ground state and excited state were as shown in **S4** and **S5** respectively.

3.5 Host-Guest Interaction

The hydrogen bond formation was confirmed in the ground state optimized structures of receptor-fluoride complexes, which has been defined as incipient proton transfer reaction from host to guest molecule. The reported experimental fluorescence quenching behaviour can be interpreted by the PET process when the fluoride anion is coordinated with APTSC. The fluorescence quenching was due to the electron transition from π-orbital of phenyl group to π -orbital of anthracene moiety. The optimized structure of receptor and receptor-fluoride complexes in the ground state and excited state suggested that the deprotonation took place at the excited state of receptor-fluoride complex, along the deprotonation happened at the N−H proton nearby the anthracene moiety. The results from TS calculations, NBO and PES analyses confirm that the deprotonation was takes place from the N-H proton, which is near by the anthracene moiety. The shifts of the signals in absorption and emission spectra are prompted to enhance the strength of host molecules and result to increase the molecular conjugation when deprotonation happens. The great difference between fluorescent properties of the sensor can be used to recognize fluoride anions. The potential energy curve structure of receptor-fluoride in the ground state and the excited state defined the bond parameter for fluoride-sensing mechanism of receptor ATSC and APTSC. The **Figure 8** shows the sensing mechanism of receptors towards fluoride ion.

4. Conclusion

In summary, we have investigated the fluoride anion sensing mechanism of ATSC and APTSC receptors. The ground state and excited state geometry of receptors and receptor-fluoride complexes have been optimized. The experimental absorption and emission spectra are well reproduced by TDDFT and vertical transition energies computed from the ground state optimized geometries. The theoretical study showed that there is an intramolecular H-bond in the receptor molecule. The fluoride ion in receptor-fluoride leads to the PET process in the relaxation of the excited states. The electron transitions are attributed from thiosemicarbazone moiety to anthracene moiety, which is the reason for the fluorescence quenching effect of receptor. The APTSC shows more quenching than ATSC, which is due to the more aromatic nature of APTSC than ATSC. The coordination of fluoride ion with N-H proton in ground state shows intermolecular hydrogen bond of N−H···F. However, the N−H proton near by the anthracene moiety attach to fluoride anion in the excited state, and results in ESPT process in the excited state to form hydrogen bond *via* N···H−F. The transition and intermediate state calculations revealed the mechanism of the host-guest interaction. The excited state proton transition mechanism of receptors towards fluoride ion were confirmed by NBO and PES analyses. The second order perturbation energy value confirms that hydrogen bonding and deprotonation takes place at the excited state of receptor-fluoride complex. In other words, ESPT in the recognition process plays an important role in designing new types of fluoride chemosensors. By comparing the results APTSC and ATSC, it is clear that the aromaticity plays key factor in fluorescent sensor for quick and efficient sensing.

Declarations

Acknowledgment

Author SMB is grateful to the RGEMS, VIT-AP University, Andhra Pradesh, India for the financial support.

Funding: No funding is supporting this manuscript

Conflicts of interest/Competing interests: We, the authors, hereby confirm that we don't have any conflict of interest in this article.

Availability of data and material: The figures, tables and other information are attached as supporting data

Code availability: Not applicable

Authors' contributions:

Dr. Sabeel M Basheer: 1st author and corresponding author. He done the computational calculations and wrote the majority of the manuscript.

Dr. Rohini Gandhaveeti: 2nd author. She is the collaborator for this work and contributed in the result and discussion section.

References

1. T.G. Jo,Y.J. Na,J.J. Lee, M.M.Lee,S.Y. Lee, C.A.Kim,A multifunctional colorimetric chemosensor for cyanide and copper(II) ions.Sens. Actuators,*B*211 (2015) 498–506.
2. J.S.Chen, P.W.Zhou, L.Zhaoab, T.S.Chu,A DFT/TDDFT study of the excited state intramolecular proton transfer based sensing mechanism for the aqueous fluoride chemosensor**BTTPB**. **RSC Adv.4** (2014)254-259.
3. C.P. Carvalho, R. Ferreiraa, J.P.D. Silva, U. Pischel,An aminonaphthalimide–putrescine conjugate as fluorescent probe for cucurbituril host–guest complexes.Supramol. Chem.25(2013)92–100.
4. G.Y.Li, D.Liu, H.Zhang,W.W. Li, F.Wang, Y.H.Liang,TDDFT study on the sensing mechanism of a fluorescent sensor for fluoride anion: Inhibition of the ESPT process.Spectrochim. Acta. Mol. Biomol. Spectrosc.149 (2015)17-22.
5. V.K.Harikrishnan,S.M. Basheer, N.Joseph, A. Sreekanth, Colorimetric and fluorimetric response of salicylaldehyde dithiosemicarbazone towards fluoride, cyanide and copper ions: Spectroscopic and TD-DFT studies, Spectrochim. Acta. Mol. Biomol. Spectrosc. 182 (2017) 160-167.
6. S.M. Basheer, J.Haribabu, N.S.P. Bhuvanesh, R. Karvembu, A. Sreekanth, Naphthalenyl appended semicarbazone as "turn on" fluorescent chemosensor for selective recognition of fluoride ion. J. Mol. Struct. 1145 (2017) 347-355.

7. J. Hasegawa, R. Miyazaki, C. Maeda, T. Ema,Theoretical study on highly active bifunctional metalloporphyrin catalysts for the coupling reaction of epoxides with carbon dioxide.Chem. Rec. 16 (2016) 2260–2267.
8. Rezaeian K, H. Khanmohammadi, Molecular logic circuits and a security keypad lock based on a novel colorimetric azo receptor with dual detection ability for copper(II) and fluoride ions. Supramol. Chem. 28 (2016) 256-266.
9. B. Zhu, L.H. Kan, H. Liu, Q. Wei, B. Du, A highly selective ratiometric visual and red-emitting fluorescent dual-channel probe for imaging fluoride anions in living cells.Biosens. Bioelectron. 52 (2014) 298–303.
10. Y. Su, S. Chai,A TDDFT study of the excited-state intramolecular proton transfer of 1,3-bis(2-pyridylimino)-4,7-dihydroxyisoindole. J. Photochem. Photobiol.A 290 (2014) 109–115.
11. S.M. Basheer, A.C. Willis, R.J. Pace, A. Sreekanth,Spectroscopic and TD-DFT studies on the turn-off fluorescent chemosensor based on anthraldehyde N(4) cyclohexyl thiosemicarbazone for the selective recognition of fluoride and copper ions. Polyhedron, 109 (2016) 7–18.
12. R.M. Duke, J.E. O'Brien, T. McCabe, T. Gunnlaugsson, Colorimetric sensing of anions in aqueous solution using a charge neutral, cleft-like, amidothiourea receptor: tilting the balance between hydrogen bonding and deprotonation in anion recognition. Org. Biomol. Chem. 6 (2008) 4089–4092.
13. S.M. Basheer, M. Muralisankar, T.V. Anjana, K.N. Aneesrahman, A. Sreekanth,Multi-ion detection and molecular switching behaviour of reversible dual fluorescent sensor.Spectrochim. Acta. Mol. Biomol. Spectrosc.182 (2017) 95–104.
14. R. Jin, W.Sun, S.Tang,A DFT study of pyrrole-isoxazole derivatives as chemosensors for fluoride anion.Int. J. Mol. Sci.*13*(2012) 10986-10999.
15. R. Jin, A.Irfan,Theoretical study of coumarin derivatives as chemosensors for fluoride anion. Comp. Theor. Chem.986 (2012)93–98.
16. H. Detert, M.Lehmann, H.Meier,Star-shaped conjugated systems.*Materials, 3*(2010) 3218-3330.
17. R.X. He, X.Y.Li,An anti-quinoid structure in dual fluorescence of fluozazene molecule and solvent effect of intramolecular charge transfer. Chem. Phys. (2007) 325–335.
18. S.M. Basheer, S.L.A. Kumar, M.S. Kumar, A. Sreekanth,Spectroscopic and TDDFT investigation on highly selective fluorogenic chemosensor and construction of molecular logic gates.Mater. Sci. Eng.C 72 (2017) 667–675.
19. O.A. Bozdemir, R. Guliyev, O. Buyukcakir, S. Selcuk, S. Kolemen, G. Gulseren, T. Nalbantoglu, H. Boyaci, E.U. Akkaya,Selective Manipulation of ICT and PET processes in styryl-bodipy derivatives: Applications in molecular logic and fluorescence sensing of metal ions.J. Am. Chem. Soc. 132(2010)8029–8036.
20. S.M. Basheer, N.S.P Bhuvanesh, A. Sreekanth,Experimental and theoretical studies of novel hydroxynaphthalene based chemosensor, and construction of molecular logic gates. J. Fluorine Chem. 191 (2016) 129–142.

21. S.M. Basheer, A.C. Willis, A. Sreekanth, Spectroscopic and TD-DFT studies on the dual mode fluorescent chemosensors based on pyrene thiosemicarbazones, and its application as molecular-scale logic devices. J. Lumin. 183 (2017) 266–280.
22. I.D. Rosal, R. Poteaua, L. Maron, DFT study of the Ring OpeningPolymerizationof ε-caprolactoneby grafted lanthanide complexes: Effect of the grafting mode on the reactivity of borohydride complexes. Dalton. Trans. 40 (2011) 11211-11227.
23. D. Udayakumari, S. Velmathi, P. Venkatesan, S.P. Wo, Anthracene coupled thiourea as a colorimetric sensor for F^-/Cu2$^+$ and fluorescent sensor for Hg^{2+} picric acid. J. Lumin. 161 (2015) 411-416.
24. T. Yanai, D.P. Tew, N.C. Handy,A new hybrid exchange–correlation functional using the Coulomb-attenuating method (CAM-B3LYP).Chem. Phys. Lett. 393(2004)51–57.
25. H. Pir,N.Günay,D. Avc, Y.Atalay,Molecular structure, vibrational spectra, NLO and NBO analysis of bis (8-oxy-1-methyl quinolinium) hydroiodide. Spectrochim. Acta. Mol. Biomol. Spectrosc.96 (2012) 916–924.
26. S. Guha, S. Saha, Fluoride Ion Sensing by an Anion-π Interaction. J. Am. Chem. Soc. 132 (2010) 17674–17677.
27. S.M. Basheer, A. Sreekanth, TD-DFT study on the fluoride and copper ion sensing mechanism of pyrene N(4) phenyl thiosemicarbazone. Comp. Theor. Chem. 1085 (2016) 31–39.

Tables

Table 1. The dominant structure parameters of APTSC and APTSC-F complex in the optimized geometries.

Bond Parameter	APTSC	APTSC*	APTSC-F	APTSC-F*
N1-H1	1.01	1.01	1.08	1.02
N2-H2	1.02	1.02	1.07	1.51
C3=N3	1.28	1.28	1.29	1.32
N3-N2	1.34	1.34	1.33	1.29
C1-N1-C2	130.90	130.05	133.58	134.05
C4-C3=N3	128.13	130.72	129.08	128.10
N2-N3-C3	122.31	122.86	121.42	119.07
C5-C4-C3-N3	115.99	139.63	121.30	159.81
C5-C4-N3-N2	34.39	10.19	2.530	32.06
S-C2-N2-N3	0.16	5.22	1.19	2.55
F-H2	---	---	1.50	0.99
F-H1	---	---	1.46	1.91
F-H2-N	---	---	153.85	163.42

Table 2. The dominant structure parameters of ATSC and ATSC-F complex in the optimized geometries.

Bond Parameter	ATSC	ATSC*	ATSC-F	ATSC-F*
N1-H1	1.01	1.01	1.01	1.01
N2-H2	1.02	1.01	1.40	1.43
C2=N3	1.28	1.30	1.29	1.32
N2-N3	1.35	1.33	1.34	1.30
C1-C2-N3	127.832	130.884	129.795	127.623
N2-N3-C2	120.884	121.043	117.114	119.735
C4-C3-C2-N3	66.059	141.483	120.043	156.869
C3-C2-N3-N2	1.248	8.725	1.837	28.680
N1-C1-N2-N3	2.242	1.673	179.21	179.60
S-C1-N2-N3	177.96	178.91	1.037	1.099
F-H2	---	---	1.05	0.99
F-H1	---	---	1.97	1.98
F-H2-N	---	---	165.99	163.56

Table 3. The low-lying absorption energies for APTSC

Energy (eV)	Wavelength (nm)	Oscillation frequency *f*	Percentage %	Composition
APTSC		-1409.49353873 A.U.		
3.3739	367.48	0.2957	100.00	H → L
3.7167	333.59	0.0014	41.67	H-1 → L+1
3.9941	310.42	0.0067	53.45	H → L+2
4.5069	275.10	0.1666	37.48	H-1 → L
4.6459	266.87	0.2275	38.84	H-2 → L+1
4.6696	265.51	0.0297	35.07	H → L+1

Table 4. The low-lying absorption energies for APTSC-F complex

Energy (eV)	Wavelength (nm)	Oscillation frequency *f*	Percentage %	Composition
APTSC–F		-1509.38713584		
3.3150	374.01	0.2795	85.78	H → L
3.7551	330.18	0.0034	35.64	H-1 → L+1
3.9613	312.99	0.0315	27.16	H → L+2
4.0145	308.84	0.0701	31.68	H-2 → L
4.4086	281.23	0.2229	27.54	H-2 → L+1
4.4764	276.97	0.0011	31.03	H-1 → L

Table 5. The second-perturbation energy E(2) (kcal/mol) of host–guest interaction with respect to receptor-fluoride complexes in ground state and excited state.

Donor (i)	Acceptor (j)	Interaction	E(2)	Donor (i)	Acceptor (j)	Interaction	E(2)
APTSC-F (Ground state)				**APTSC-F*** (Excited State)			
CR F	BD* N25-H41	σ-σ*	2.14	CR F	LP* H41	n-σ*	11.71
LP F	BD* N27-H42	n-σ*	8.78	LP F	LP* H41	n -n*	12.69
LP F	BD* N25-H41	n-σ*	28.52	LP F	LP* H41	n-n*	352.76
LP F	BD* N27-H42	n-σ*	44.42	LP F	LP* H41	n-n*	3.30

Figures

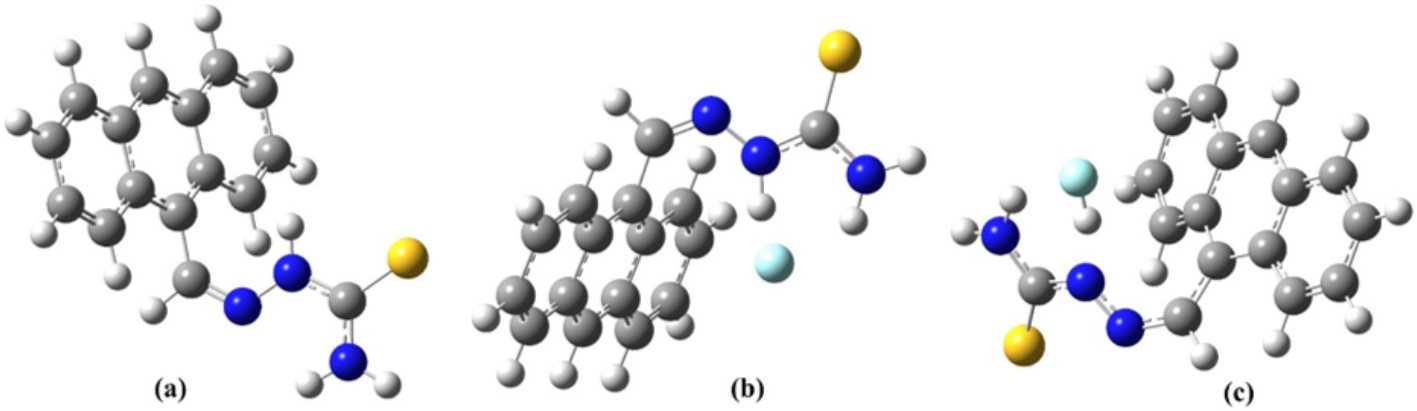

Figure 1

Optimized structure of (a) ground state ATSC, (b) ground state ATSC-F complex and (c) excited state ATSC-F complex.

Figure 2

Optimized structure of (a) ground state APTSC, (b) ground state APTSC-F complex and (c) excited state APTSC-F complex.

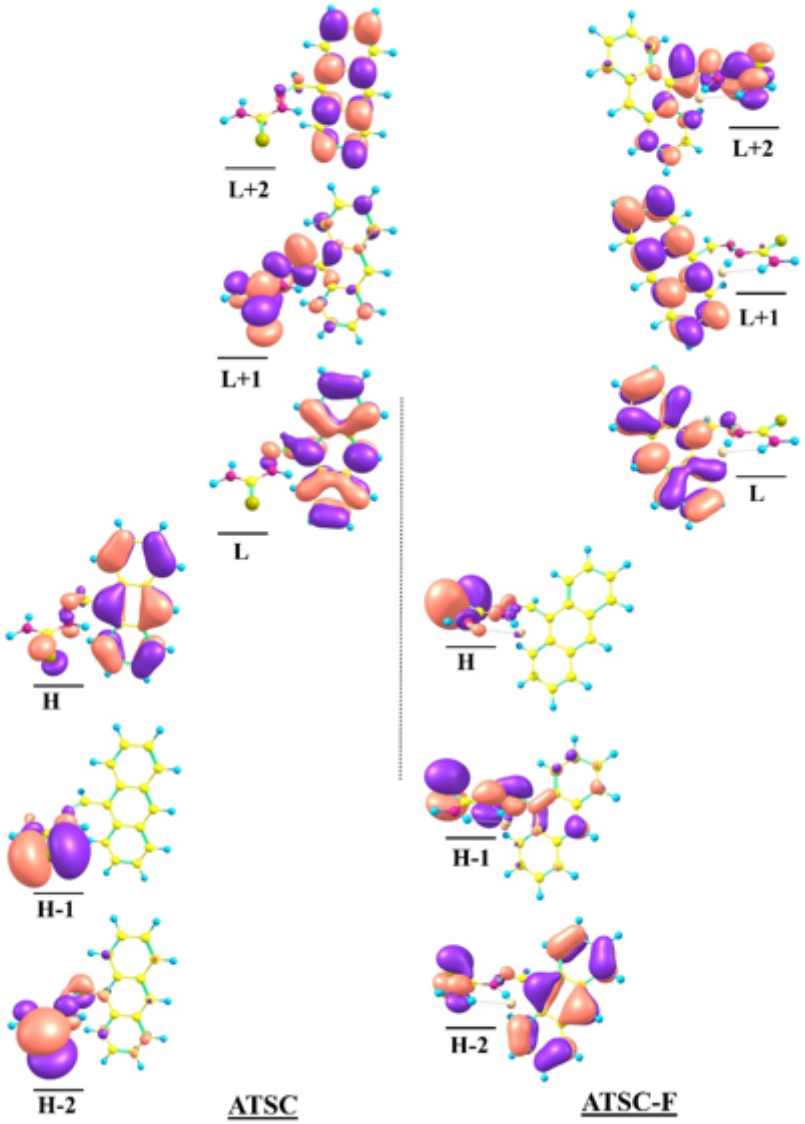

Figure 3

The dominant molecular orbital transitions of ATSC and ATSC-F complex

Figure 4

The dominant molecular orbital transitions of APTSC and APTSC-F complex

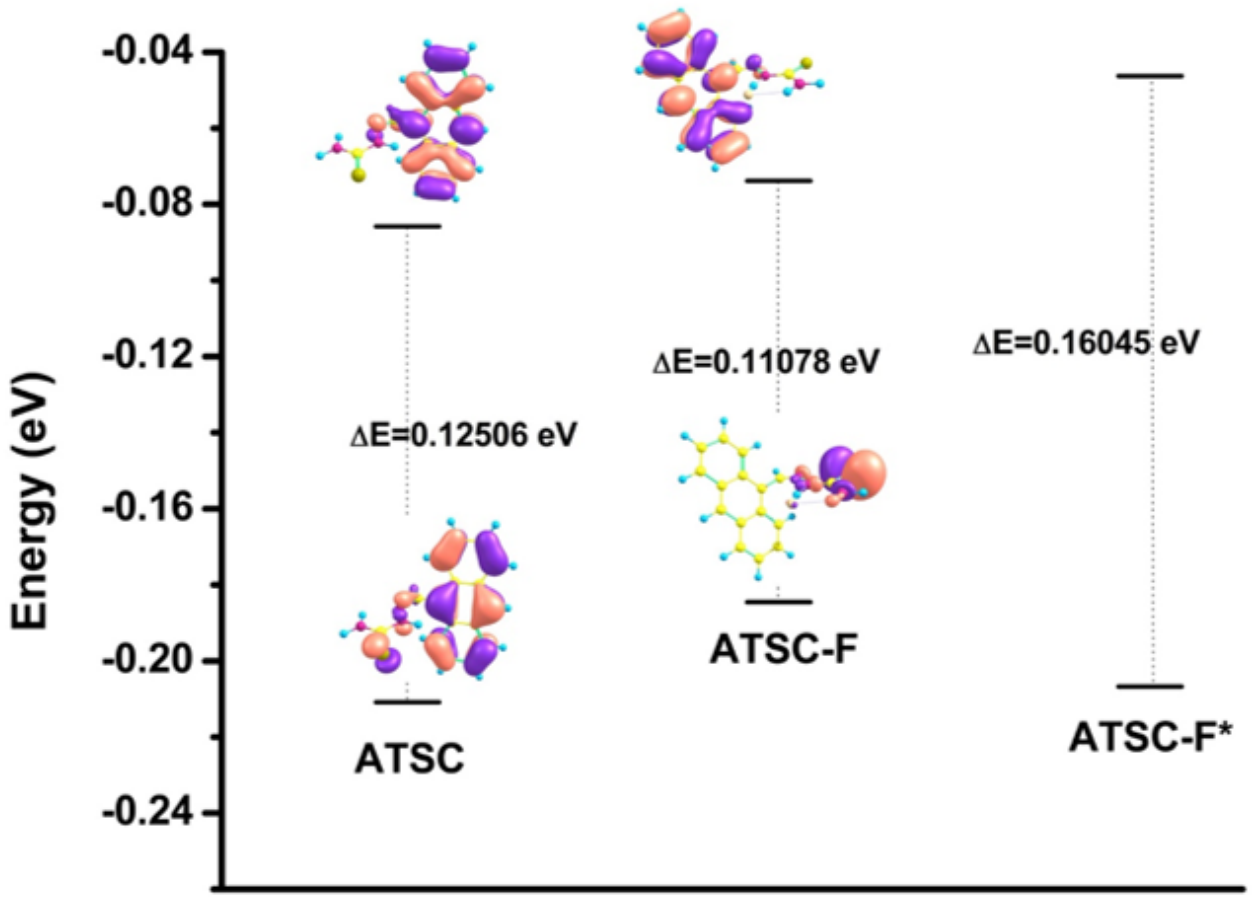

Figure 5

The energy gap between HOMO and LUMO orbitals of ATSC, ground state ATSC-F and excited state ATSC-F complex

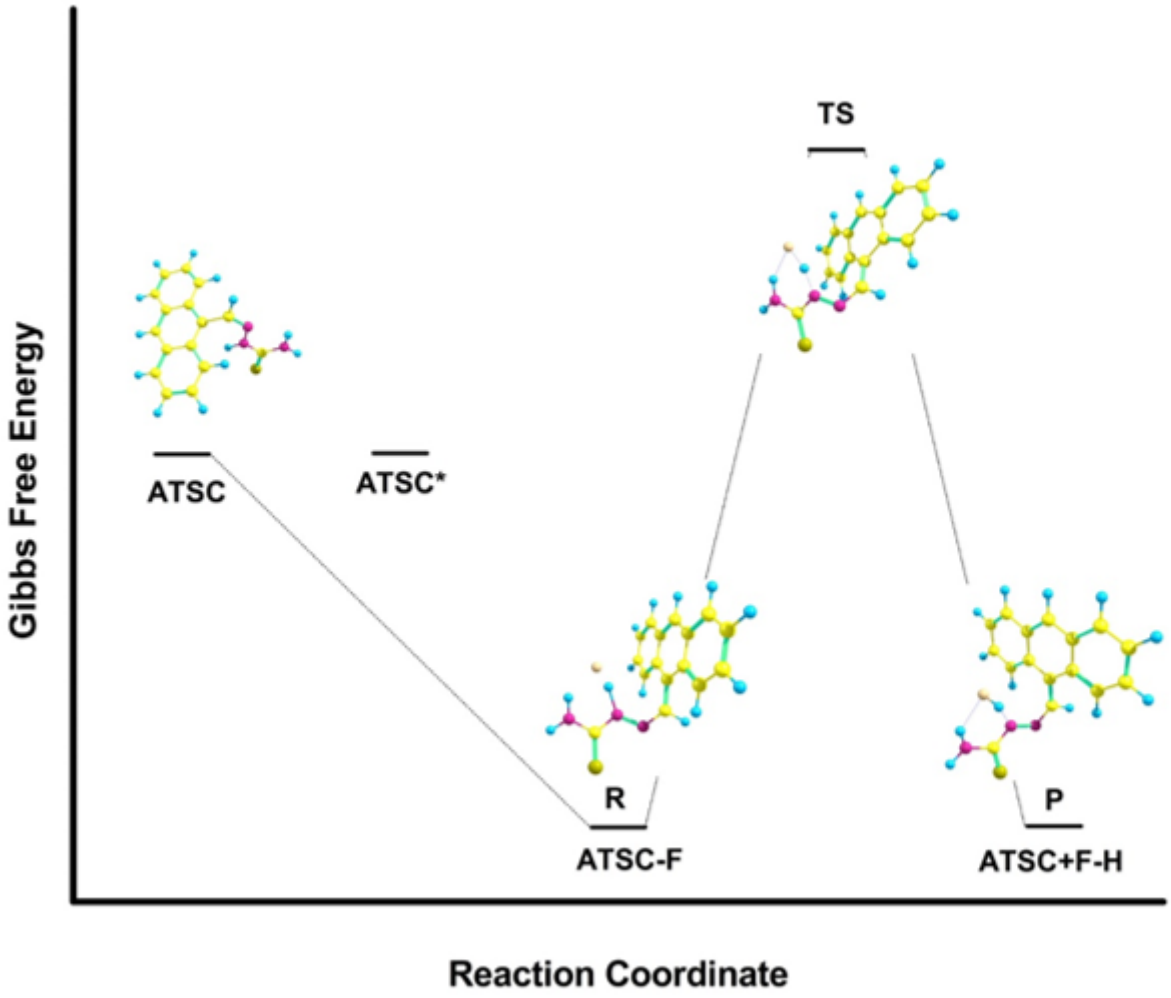

Figure 6

Gibbs free energy profile of the fluoride sensing mechanism of ATSC [R=Reactant; TS=Transition State; P=Product]

Figure 7

Gibbs free energy profile of the fluoride sensing mechanism of APTSC. (B: APTSC; B*: Excited state APTSC; B+F: APTSC-F(R=Reactant); (TS=Transition State); B+F-H: Excited state APTSC-F (P=Product)

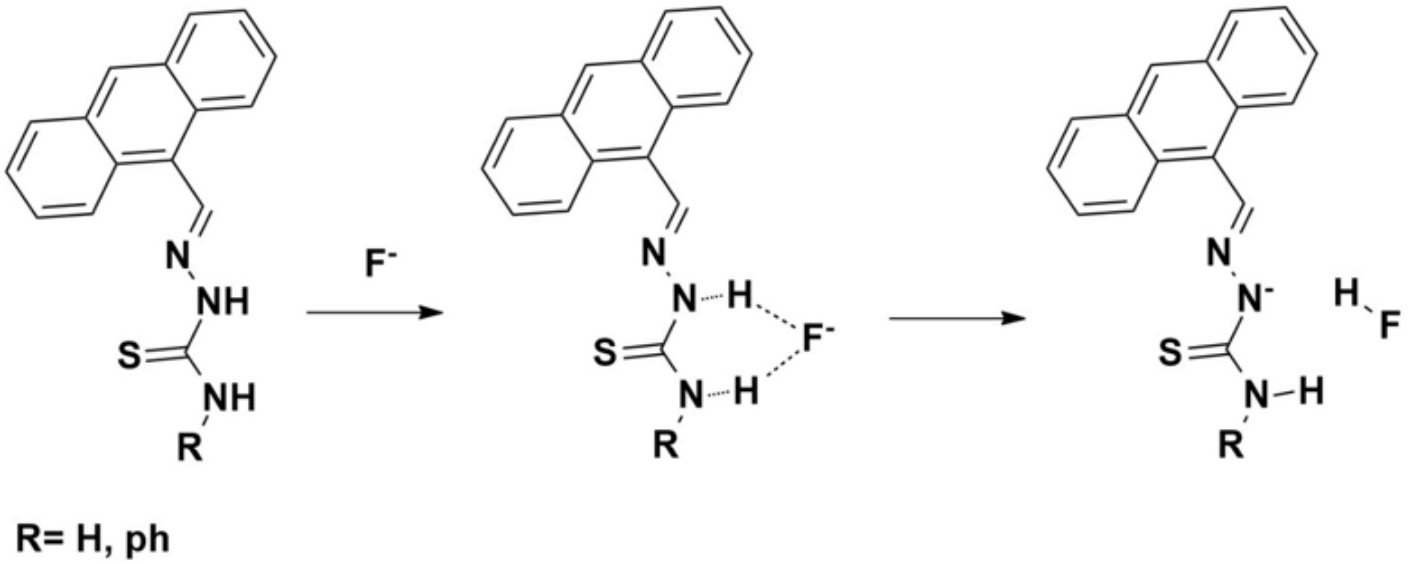

Figure 8

Proposed sensing mechanism of ATSC and APTSC with fluoride ion. Dotted line denoted hydrogen bond.

Supplementary Files

This is a list of supplementary files associated with this preprint. Click to download.

- GraphicalAbstract.docx
- SupportingData.docx